SAND2014-20012C

SPECTROSCOPIC TEMPERATURE INFERENCES FROM DOWNWARD BURNING SOLID ROCKET PROPELLANTS

D.M. Surmick and C.G. Parigger
University of Tennessee Space Institute
Tullahoma, TN

A.D. Haug and A.B. Donaldson
New Mexico State University
Las Cruces, NM

W. Gill
Sandia National Laboratories
Albuquerque, NM

ABSTRACT

The plume temperature of a downward burning aluminized solid rocket propellant is determined using spectroscopy methods as a function of the radial position, the substrate surface the plume is incident upon, and the gap distance between the propellant and substrate. The temperature of the plume is expected to be affected by separate contributions from gas, aluminum particle, and soot components in the plume. It is of interest to determine the temperature of burning aluminum particles and the flame temperature. The aluminum particle temperature is inferred by fitting diatomic molecular aluminum monoxide emissions to theoretically calculated spectra. Theoretical molecular spectra are calculated from accurately compiled line strength tables. The fitting of experimental to theoretical spectra is accomplished with the use of a Nelder-Mead algorithm. The flame temperature is evaluated using records of broadband spectral emissions from the thermal continuum radiation. Temperatures are determined by fitting the broadband spectral emissions to a semi-logarithmic representation of Planck's radiation law. Constant, $1/\lambda$, and $1/\lambda^2$ emissivity models are applied in the evaluation of the flame temperature. The substrate materials studied were high insulated carbon, graphite, FlexFram, and wet concrete. The flame temperatures are found to typically vary between 2200-2500 Kelvin depending on gap size, substrate material, and distance from the propellant. The AlO emission temperatures are found to be in the 2800-3200 Kelvin range.

INTRODUCTION

The temperature of a solid rocket propellant plume is of considerable interest for characterizations of launch pad and pay load safety due to lack of models and supporting experimental data that describe combustion of solid rocket propellants during off design burns. Aluminum is a common component in solid rocket propellant motors due to the favorable material properties of aluminum which provide a method to control the burn rate of the propellant and increase the energy of the burn. The burning propellant at ambient atmospheric conditions, analogous to those encountered during an aborted launch scenario, is not well understood and, as such, models of aborted launch scenarios with experimental support are needed. During an aborted launch it is possible for the propellant to break apart and impact launch pad and pay load surfaces. As a result there is special importance to determining the propellant plume characteristics for combustion at atmospheric pressure, where one of the key parameters is the

temperature distribution in the plume. The goal of this study is to use optical spectroscopy of the plume that shows discrete and continuous emissions to infer the temperature in simulated scenarios where a piece of propellant would be incident on a launch pad surface.

The plume itself is expected to indicate three temperatures due to the separate contributions from the gas, aluminum particles, and alumina soot components that are present. Determining the temperature distribution provides insight into the dynamics of the propellant combustion for different regions of the plume, where particular interest is paid to the region above the simulated launch pad surface. Optical emission spectroscopy is a preferred method for determining the temperature of the plume since it offers a relatively non-invasive method to probe the interior of the propellant plume. Further, optical observations of the plume are also relatively easy to implement in experiments. Diatomic molecular aluminum monoxide (AlO) emissions are used to infer the plume temperature from discrete molecular transitions. The source of the AlO is oxidation of individual aluminum particles in the plume. Studying the temperature determined from AlO emissions allows one to gain insights into the dynamics and temperature of burning aluminum particles within the propellant plume.[1] Spectroscopic measurements of AlO are often used as a diagnostic for determining the temperature of aluminum containing combustion events because AlO is the first transient product in the oxidation of aluminum to alumina.[2] Spectroscopy of AlO is frequently used in this application due in part to the strong observational presence of the AlO $B^2\Sigma^+ \rightarrow X^2\Sigma^+$, blue-green spectroscopic signature in the 420-560 nm wavelength range and the availability of spectroscopic instruments with high sensitivity in the wavelength region of interest.[3,4,5] Temperatures inferred from an aluminized combustion event typically show large temperature ranges from 2400 up to 4000 Kelvin.[6,7,8] Moreover, other characteristics of aluminum particle combustion are of interest in studies of aluminum combustion, such as flame propagation speeds and gas atmospheric effects.[9,10] Further, many studies have not been performed with large scale propellant burn experiments. When reviewing the broad range of temperature values available in the literature, one finds the complex nature of aluminum particle combustion, and consequently, the continued need for experimental determination of aluminum particles burning in the propellant plume.

The flame temperature is expected to show thermal continuum emission characteristics due to broadband radiation of heated particles and bulk material from the propellant plume. Further, the propellant plume is known to consist of several small particle components from individual aluminum particles and of the alumina soot particles. The temperature from these particle contributions can be represented by the broadband thermal continuum radiation. Wavelength dependent emissivity models have also been shown to provide insight into the temperature distribution of aluminized flames composed of small particles.[11,12,13] The temperatures determined in the previous studies also show a temperature range of 2600 to 3000 Kelvin for black-body emission models and similar ranges for wavelength dependent emission models. These studies are concerned with aluminized flames in general rather than aluminized solid rocket propellants, specifically. This effort specifically employs a probe inserted into a downward burning propellant to simultaneously measure continuous and discrete spectroscopic emissions to determine the temperature of the plume as a function of the substrate material the plume is incident upon, the gap distance between the propellant and substrate material, and the radial position within the plume.

EXPERIMENTAL DETAILS

This study quantifies the temperature distribution of the plume emanating from a downward burning solid rocket propellant from measured broadband continuum and discrete AlO emission spectra. To this end, an experiment was devised in which a probe was physically placed and systematically moved in a downward propellant plume. The emission spectroscopy measurements and temperature inferences that are reported in this work were simultaneously arranged with several other experiments as part of a large scaled test series of solid rocket

propellant combustion and propellant plumes.[1] Other experimental devices fielded during this test series to infer the temperature of the plume included thermocouple, infrared Fourier Transform spectroscopy, and fan beam emission tomography measurements. The overall goal of the experiments was to determine the temperature as a function of simulated launch pad surface and gap distance between the propellant surface and the substrate material used to simulate the launch pad surfaces. The investigated substrate materials were wet concrete, graphite, highly insulated carbon (HI Carbon), and FlexFram. The gap distances between the substrate materials and bottom surface of the propellant that were considered were 1, 1.5, and 2 inches. For each test, the gap distance was held constant using an X-ray source and detector to measure the position of the propellant surface. The propellant diameter size was also examined, with propellant sizes ranging from 6 to 20 inches in diameter. Several experimental configurations and combinations of substrate material, gap distance, and propellant diameter were considered throughout the test series.

For the observation of line-of-sight measurements of optical emission spectra within the plume, a probe was introduced into the plume and its position was systematically varied to measure spectra from specific plume regions. The experiments were performed in a 20 by 20 foot chamber that was open to ambient, atmospheric conditions, *i.e.*, atmospheric pressure and temperature. The chamber was vented from the bottom so that smoke could be purged from the chamber through a chimney. The probe consisted of a steel pipe attached to a stepper motor. The stepper motor moved the probe in regular intervals along a horizontal track. One end of the steel pipe was inserted into the plume to record data with a collimating lens coupled to a bifurcated fiber optic cable. The collimating lens and optical fiber were attached to the pipe. The spectroscopic equipment was protected with ablative and reflective thermal shielding so that the only part of the equipment that was exposed to the propellant plume was the steel pipe probe. Figure 1 shows a diagram of the arrangement inside the combustion chamber used to collect the emission spectra for this work. Figure 1 also shows the other instrumentation fielded simultaneously to the optical emission spectroscopy equipment. The dark blue rectangle represents the table used to hold the stepper motor and track and is also indicated with the red arrow. The line originating from the rectangle represents the steel pipe probe.

The spectra were recorded with two Ocean Optics fiber-coupled spectrometers. One of the spectrometers was selected with narrowband sensitivity in the wavelength region of 420-560 nm, while the other was selected with broadband sensitivity in the wavelength region of 200-1100 nm. The average spectral resolution was 0.5 nm for the narrowband spectrometer and 0.75 nm for the broadband spectrometer. The purpose of the narrowband instrument was to collect aluminum monoxide emission spectra to infer the temperature of the diffusion flame surrounding aluminum particles in the propellant plume. The purpose of the broadband instrument was to collect thermal continuum radiation from the propellant plume to infer the flame temperature. The amount of distance traversed by the steel pipe varied in the experimental matrix. Distances from the edge of the propellant ranged from 2 to 13 inches, with an average spacing between measurements of approximately 0.1 inches. Prior to detailed analyses, all recorded spectral data were wavelength calibrated and intensity calibrated for detector and background sensitivity.

SPECTRAL FITTING

For the determination of the temperature distribution in the propellant plume from optical emissions, AlO spectra were fit to theoretical calculations of AlO emissions using the diatomic molecular theory. The continuum thermal radiation was interpreted with Planck's radiation law including consideration of wavelength dependent emission models for evaluation of the flame temperature.

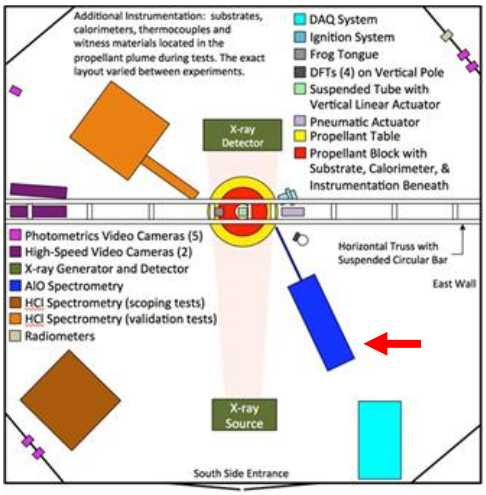

Figure 1. Top view of the location of the instruments during a propellant test. Spectrometers for AlO and background continuum emission measurements were located at the position of the dark blue rectangle, also indicated by the red arrow at lower right of the schematic for the experiments.

ALUMINUM MONOXIDE FITTING

For the AlO temperature determination, the experimental spectra are fit to theoretical calculations of the AlO $B^2\Sigma^+ \rightarrow X^2\Sigma^+$ blue-green transition. The AlO spectra are computed from accurately compiled line strengths.[14,15] Detailed accounts of the calculation of the theoretical AlO spectra used in this work are given in References 14 and 15 and application of the line strength tables to AlO spectra collected from propellant plumes is further described in detail in References 1,16, and 17. The comparison between experimental and theoretical spectra is made with the use of a Nelder-Mead nonlinear fitting algorithm. The Nelder-Mead algorithm formalizes an optimization technique in which a geometric simplex is created and reduced in size until a specified tolerance level is reached.[18,19] The size of the simplex is determined by the number of free or varied parameters in the fitting. The number of vertices the simplex has is one more than the number of the free parameters. This algorithm is chosen for its performance in comparing measured and predicted spectra with multiple parameters simultaneously. The parameters that were minimized for each fit were the temperature, spectral resolution, *i.e.*, the FWHM of measured lines in a molecular transition, and a variable baseline offset. A disadvantage of the Nelder-Mead algorithm is that it requires a reasonable initial seed (within an order of magnitude) for the fit parameters of interest. However, during fitting, the Nelder-Mead typically returns the first local minimum it encounters, as determined by the selected tolerance, rather than a global minimum. Sufficient choice of the input parameter's initial seeds and the algorithm tolerance allow one to infer temperatures with physically significant but possible systematic errors originating from the fitting algorithm, even when good initial seed parameters are introduced at the starting point.

For fitting of AlO spectra, quadratic baseline offsets were considered as well. The offsets were found to be nearly linear in nature for most cases. This was expected, given the AlO emissions are superimposed with the thermal continuum background emissions over a relatively small (less than 100 nm) wavelength region. Though the spectral resolution is a largely determined quantity from the physical limitations and settings in a given experiment, it can be varied as a method to determine the error of the AlO temperature from the wavelength response of the detector, and further, it can provide insight into potential systematic errors associated with the fitting algorithm. While both spectrometers were employed to record AlO emissions, the narrowband instrument was the primary source for AlO temperature inferences due to the greater sensitivity of the instrument in the 460 to 530 nm wavelength range. The average spectral resolution of this instrument is 0.5 nm, and as such, values of 0.35 and 0.65 nm were used to

over- and underestimate the resolution. The variation of 0.5 ± 0.15 nm was determined by varying the spectral resolution parameter over several iterations of a particular fit. Results of sample fit for an AlO spectrum is illustrated in Figure 2 for a propellant burning onto a graphite substrate measured 3 inches from the propellant edge. The inferred temperature for this position was 2969 ± 93 Kelvin. Noticeable in the figure is the decreased instrument sensitivity (green curve) in the 460 to 480 nm range. Though the AlO contributions are significantly diminished in this region, it was included in the fit to infer a proper background. Excluding this region would lead to poor background inferences and much larger determined temperatures, often as high as 4000 Kelvin. This observation indicates that variations in the baseline offset have a significant impact on the overall systematic error inherent to the fitting algorithm. Though systematic errors resulting from fitting the baseline offset have not been systematically investigated in the current study, the errors are expected to be similar in magnitude to those found in the evaluation of errors due to variation of the spectral resolution.

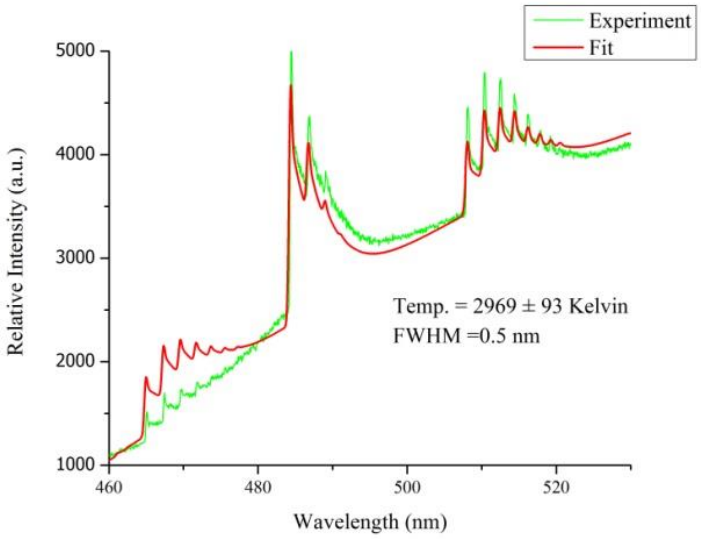

Figure 2: Experimentally recorded and fitted AlO propellant spectra burning onto a graphite substrate at 3 inches from the propellant outside edge of the propellant diameter.

THERMAL CONTINUUM FITTING

The temperatures of the flame and also the alumina smoke are determined from spectroscopic measurements of the propellant plume. The data from recorded broadband emissions in the 500-950 nm wavelength range were utilized in this analysis. The flame is thought to be in equilibrium with the alumina smoke emanating from the propellant plume. The wavelength region for the analysis is correlated with the sensitive range of the broadband spectrometer that was primarily used to infer the flame temperature. The sensitive range was initially taken from the spectrometer's specifications but also determined from performing detector background sensitivity calibrations. The recorded continuum emissions in the plume are expected to originate from the thermal continuum of the flame and as such are expected to follow Planck's radiation law. Due to presence of particles of relatively small size in the flame, different emissivity models are considered in conjunction with Planck's law. The emissivity describes the ratio of actual power emitted to the power emitted by a black-body radiator and, as such, an emitting source following a black-body emission model will have a constant emissivity of one, $\varepsilon = 1$. So called grey emitters in the plume, such as large aluminum agglomerates and alumina soot particles, will have constant emissivity that are less than one as black-body radiation represents an ideal emission model. The difference between grey and black-body emissions is expected to be relatively small for the propellant plume and, as such, the black-body emission model is utilized. When the size of an emitting body is on the order of the wavelength of light being

emitted, it is possible for the emissivity to become wavelength dependent, *i.e.*, $\varepsilon = \varepsilon(\lambda)$, that can be described within a classical Lorentz oscillator model.[21] In this work, three emissivity models are considered: 1) Black-body emission; 2) $1/\lambda$ wavelength dependent emissions; and 3) $1/\lambda^2$ wavelength dependent emissions. The source of the $1/\lambda$ dependency is from molten aluminum agglomerates, and the $1/\lambda^2$ is due to presence of micron sized or smaller alumina particles.[16,17] Detailed descriptions of the source for these models are provided in References 22 and 23 where Wien's law is formulated for wavelength dependent emitters and a description of application of such results is given in References 16 and 17.

The resulting effect from considering a wavelength dependent emission model is a modified Wien's constant which corresponds to a lowered temperature for a similar wavelength of maximum emissions. For blackbody radiation Wien's constant is 2.898×10^6 nm-K. The corresponding Wien's constant for $1/\lambda$ and $1/\lambda^2$ dependent emissions are 2.415×10^6 nmK and 2.070×10^6 nmK , respectively. To further illustrate the effect, consider a black-body emitter with a maximum wavelength emission of 1000 nm which has a corresponding emission temperature of 2898 Kelvin. Wavelength dependent emissivity models will have temperatures of 2415 and 2070 Kelvin for $1/\lambda$ and $1/\lambda^2$ emissions, respectively. This temperature lowering effect is illustrated in Figure 3.

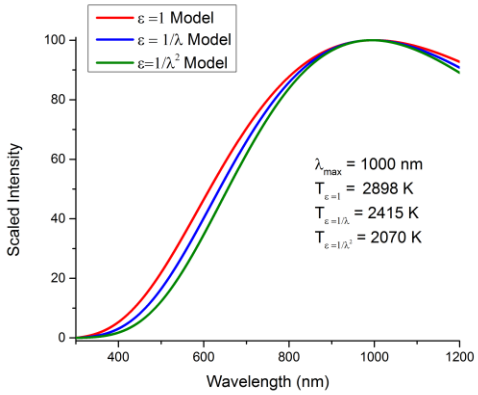

Figure 3. Thermal emission curves for ϵ = 1, 1/λ, and 1/λ^2 emissivity models with a fixed maximum wavelength emission of 1000 nm.

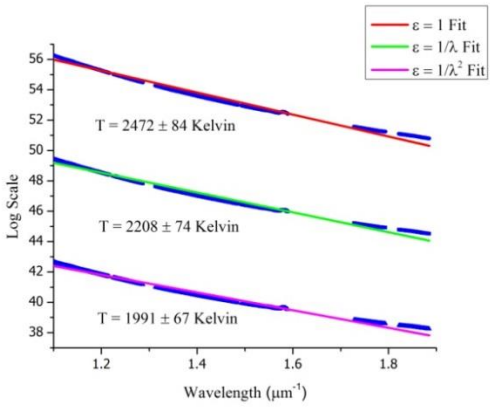

Figure 4. Planck fitting results for a downward burning propellant onto a graphite substrate 3 in from the propellant edge.

The maximum wavelength emission for the spectra observed from the propellant is expected to be in the 1000-1300 nm range. Given the decreased sensitivity of the broadband spectrometer in the 1000 nm wavelength region, the limited wavelength range of the instrument, and the expected temperatures from propellant plume, direct fitting of the measured peak from broadband spectra by application of Wien's displacement law (with wavelength dependent emission models to determine the wavelength of maximum emission) is not used for determining the flame temperature. In order to extract the flame temperature from the thermal continuum, Planck's law is directly applied to the recorded data by fitting a semi-logarithmic version, within the indicated approximation in Equation (1) below, of the Planck equation to the experimental data.[16,17] The approximation is introduced as follows

$$\ln\left(C\ \frac{I(\lambda,T)\ \lambda^5}{\varepsilon(\lambda)}\right) = -\ln\left(\exp\left[\frac{hc}{k_B}\frac{1}{\lambda T}\right]-1\right) \cong -\frac{hc}{k_B}\frac{1}{\lambda T}. \qquad (1)$$

Here, *C* is a constant, $I(\lambda,T)$ is the recorded intensity, and $\varepsilon(\lambda)$ indicates the emissivity model. Using this fitting method, the natural logarithm of the collected data multiplied by λ^5, λ^6, and λ^7 for constant, $1/\lambda$, and $1/\lambda^2$ emissivity models, respectively, are plotted versus the inverse wavelength

and are fit using linear least squares methods. The slope of the fitted line is used to determine the temperature by way of Equation (1). This type of analysis is applied only to the continuum recorded with the broadband spectrometer. Though the narrowband instrument recorded both AlO and thermal continuum emissions, the AlO emissions dominate the recorded spectra. A relatively small continuum background for fitting remains after the AlO emissions have been properly subtracted from the recorded data. A typical fit of this kind is shown in Figure 4 which corresponds to the same propellant burn shown in Figure 4 for AlO emissions. Contributions from atomic and molecular spectral emissions that could be identified have been omitted to reduce the error of the straight line fit. Such emissions are AlO, sodium, potassium, aluminum, and iron. The inferred temperatures in Figure 4 are 2472 ± 84, 2208 ± 74, and 1991 ± 67 Kelvin for constant, $1/\lambda$, and $1/\lambda^2$ emissions, respectively. The errors are estimated from the determined error of the slope associated with the linear least squares fitting. The indicated errors also include the three percent error introduced from use of the approximation in the wavelength region of interest.

RESULTS AND DISCUSSION

The propellant tests were designed to investigate the effects of: 1) gap height between the propellant, 2) the substrate and 3) the type substrate material the plume was incident upon. For the study of emission spectra from the plume, the temperature of the plume was the parameter of interest. During testing, a series of scoping model (SM) tests were performed to fine tune the experimental methods used during a second series of verification model (VM) tests. Temperatures were inferred from AlO and broadband spectral measurements in both tests. Figure 5 shows a summary of the determined temperatures from both the AlO fitting, and it also shows results of fitting of the three considered thermal emission models from the SM test series. Figure 6 shows the results from the VM test series. Missing temperatures from each of the two figures for any of the fitting methods indicate poor temperature inference due to a low signal to noise ratio.

As can be seen from Figures 5 and 6, the temperatures across each of the test series appear to be consistent, (apart from some outliers such as the test performed from VM-6) in the sense that the aluminium oxidation is expected to be at a higher temperature than the surrounding alumina particles (which should be in thermal equilibrium with the gas due to the submicron particle size). This indicates that the gap size and propellant diameter do not have a significant effect on the plume temperature. It should be noted, however, that all of the spectral measurements made in this study were preformed outside of the propellant, not under it. This was due to the size of the steel pipe probe used and the gap heights under investigation. These measurements were conducted at the same height of the gap such that the gap would be in the probe's field of view given an optically thin propellant plume. With this in mind, it is likely that the spectral measurements made in this study would not give proper insight into the effect of the gap of the propellant plume. This is understood to be particularly true for the flame temperature inferred from the thermal continuum. Whereas the aluminum particles are expected to be the same temperature regardless of the plume region where particles are located, the flame temperature is expected to display a difference for the differing flame regions outside of the gap versus inside the gap due to boundary conditions. The observed null result for the gap height effect should be considered within this context when comparing to other temperature determinations that measured the temperature field in the gap between the propellant and the substrate. Typical thermal continuum temperatures from both the SM and VM series are found to be in the 2200-2500 Kelvin range with typical errors falling into the 65-80 Kelvin range, while the AlO temperatures have a range of 2750-3200 Kelvin with typical errors in the 100-150 Kelvin range.

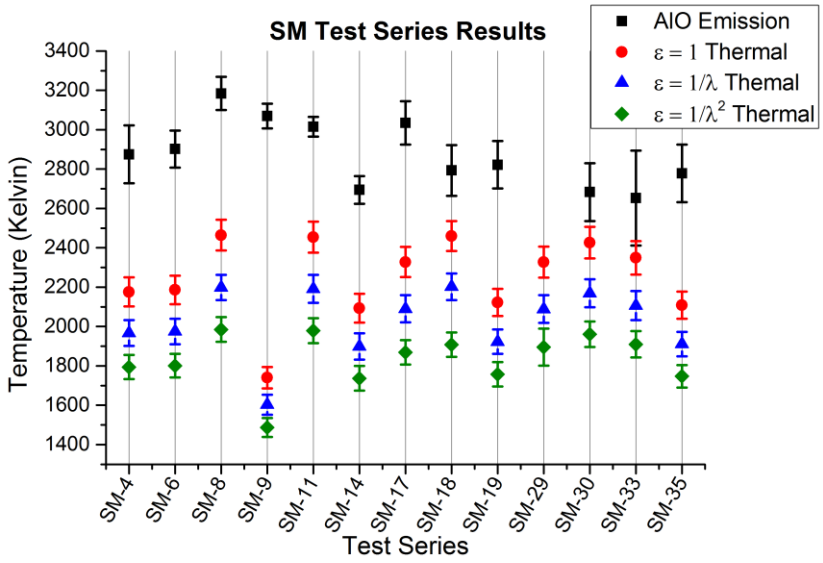

Figure 5. Temperatures for AlO and thermal continuum emissions for the scoping model tests.

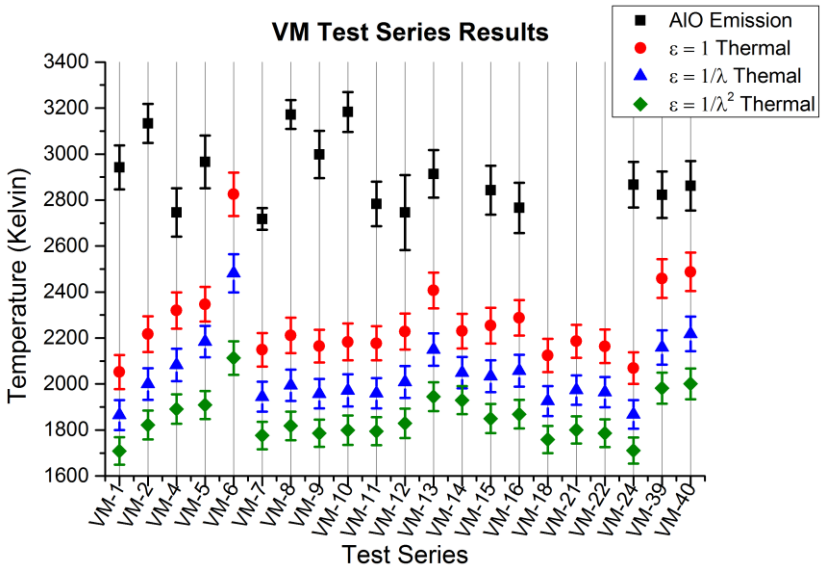

Figure 6. Temperatures for AlO and thermal continuum emissions for the verification model tests.

For each test, the radial position was varied in the range of 1-2 inches outside the outer diameter of the propellant charge. As well, the position was varied from each test which varied from as close as 2 inches to the propellant to as far as 14 inches from the propellant edge. Figure 7 depicts the radial dependence of the temperature for two VM series tests with FlexFram (VM-15) and HI Carbon (VM-24) substrates for initial positions of 4 and 6 inches from the propellant outer diameter, respectively. The two plots show that there is a very slight positional dependence to the temperature, particularly for the thermal emissions when properly considered with the given error bars. The AlO temperature shows a variation without a trend within the 2800-3200 Kelvin temperature range. Figure 8 shows the temperature as a function of the radial position for a single test series with a HI Carbon (VM-40) substrate made at initial positions of 2.1 and 10.1 inches from the propellant outer diameter. Similarly, the inferred temperatures within each test show a slight variation. The overall temperature difference between the closest measurements to the farthest measurements is approximately 175 Kelvin for the thermal temperature inferences,

but, when considered with the typical error of ± 70 Kelvin, the 175 Kelvin discrepancy is all but covered by a single temperature. Again, there is no apparent trend in the temperature from the AlO fits, just a similar range of temperatures of 2700 to 3000 Kelvin is found. As such, a single temperature is found to represent each fitting method/model in Figures 7 and 8 below. The radial positions were chosen based on survival of the tube which was inserted into the radial outflow of gases and particles emanating from the gap.

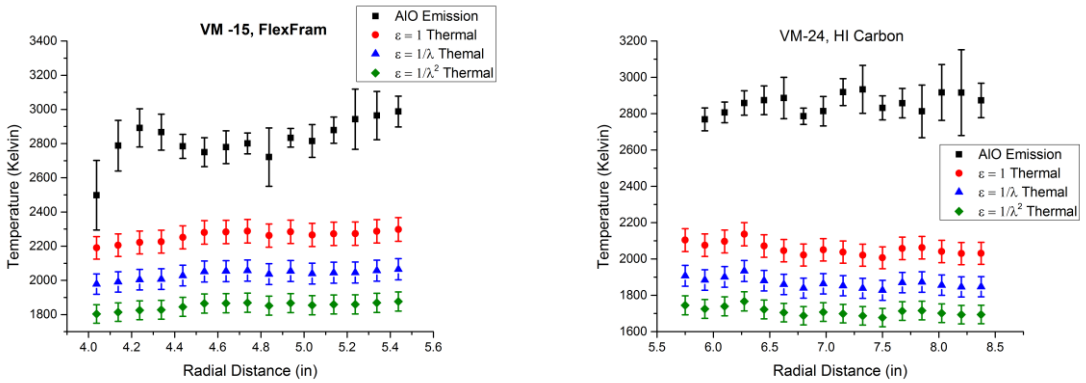

Figure 7. AlO and thermal emission temperature radial dependence for VM-15(left) and VM-24(right) tests.

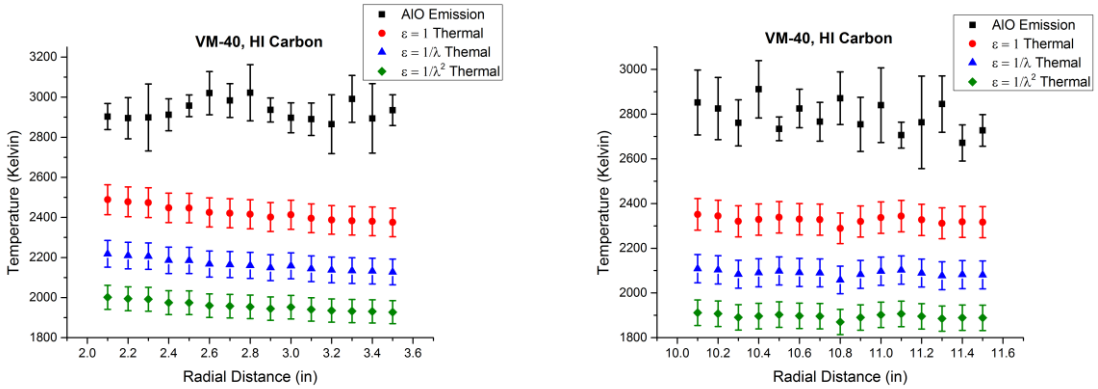

Figure 8. AlO and thermal emission temperature radial dependence for the VM-40 test for initial radial positions of 2.1 inches (left) and 10.1 inches (right) .

Figure 9 shows temperature results from the VM test series for the HI Carbon, graphite, and FlexFram substrates and the SM test series wet concrete substrate. The VM series did not yield useable data from any of the wet concrete tests and as a result the SM series was used to provide insight on the temperature substrate dependence for wet concrete. The results shown in Figure 10 again confirm that the temperatures found from the AlO emissions do not prescribe to any trend and are, again, found to be in the 2800-3200 Kelvin range. Comparison of the thermal temperatures from each substrate shows a similar temperature range without an apparent trend. This range is 2200 to 2500 Kelvin. The HI Carbon and graphite substrates appear to have a tendency to lie at the upper part of this range while the FlexFram substrate appears to lie toward the lower end of this range. The temperatures inferred from this study are similar to those found in a recent study performed with an upward burning propellant where the temperature was found to increase as a function of distance from the propellant surface.[16,17,24] AlO emissions resulted in temperatures between 2600 and 2900 Kelvin while thermal continuum emissions showed temperatures between 2400 and 2700 Kelvin at a height of six inches above the propellant

surface. In the previous investigations, a similar style probe was inserted and passed through the interior of the upward burning propellant plume.

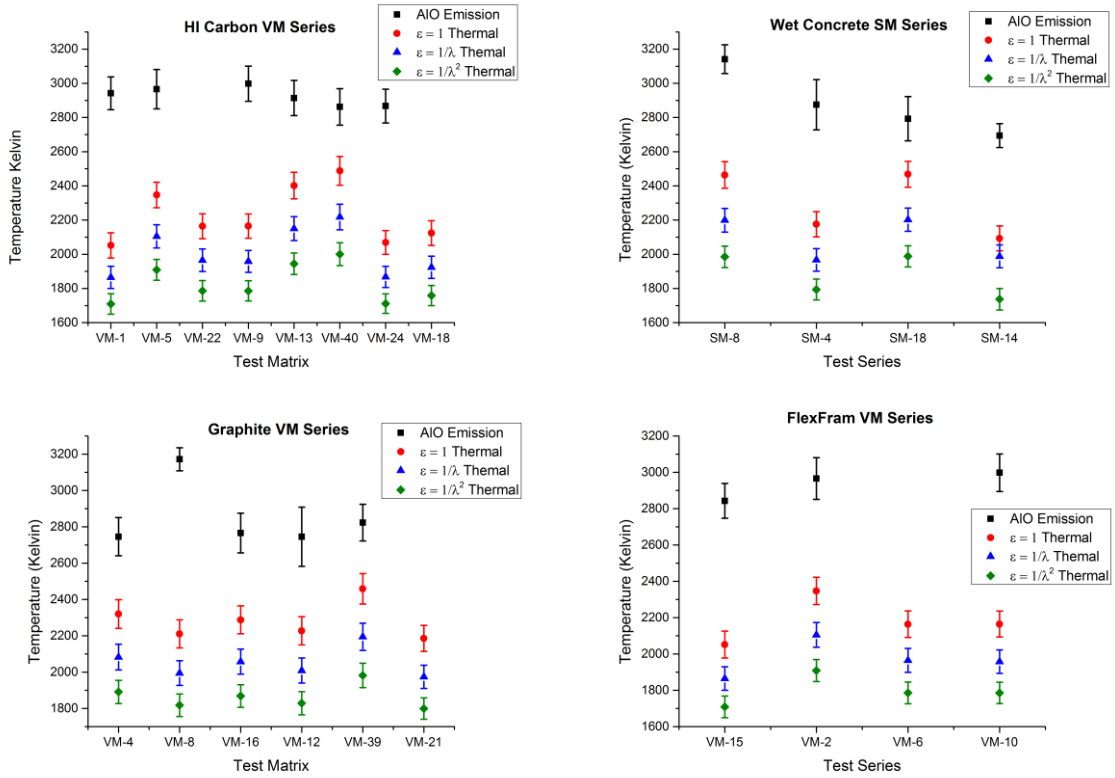

Figure 9. AlO and thermal emission substrate dependence for the HI Carbon (top left), wet concrete (top right), graphite (bottom left), and FlexFram (bottom right) substrates.

The temperature results in Figure 9 also show that there is some evidence for use of differing wavelength dependent emission models. This can be seen as the close agreement in the VM-22 and VM-9 black-body temperatures with the VM-13 and VM-5 $1/\lambda$ temperatures for the HI Carbon substrate and as well as the SM-4 black-body and SM-18 $1/\lambda$ temperatures from the wet concrete substrates. Matching of temperatures from different emissivity models would indicate that the particle size has an effect on the thermal emission. The alumina smoke particle size is expected to be on the order of one micrometer or less in diameter, while molten aluminum agglomerates may range in size from a few microns to hundreds of microns in diameter.[5,25] A thorough investigation of the wavelength dependency of the emissivity model based particle size is required before any further inference can be made on the wavelength dependency of emissions within the propellant plume. It is also likely that a $1/\lambda^n$ model will need to be considered. This assertion is supported by the findings of a recent treatment on the wavelength dependence of combusting aluminum nanoparticles,[7] where the *n* parameter was found to lie between 1 and 2. However, this finding would indicate the need for continued detailed study of the emission of small particles, particularly in the propellant plumes.

SUMMARY AND CONCLUSIONS

The temperature of a downward burning propellant plume has been evaluated as a function of the separation of the propellant from the incident substrate material, the substrate material exposed to the plume, and the radial position of the plume exterior to the gap. The temperatures were determined by analyzing discrete AlO and thermal continuum emissions. AlO emissions were fit to theoretical spectra calculated from accurately compiled line strength tables. The fitting was accomplished with a Nelder-Mead algorithm. The AlO temperatures showed no apparent trend as a function of gap size, substrate material, or radial position and were found to be in the 2800-3200 Kelvin range. The thermal continuum temperature was deduced by fitting a semi-logarithmic version of Planck's radiation law for black-body, $1/\lambda$, and $1/\lambda^2$ emission models. These results also showed that there was no correspondence between the gap height, substrate material, and radial position and the inferred temperature. The temperature range for the reported measurements was 2200 to 2500 Kelvin. Further investigation of the wavelength dependency of the thermal continuum emission model is required: a benchmark study should be completed for combusting alumina and for aluminum particles of varying sizes. The temperatures inferred in this study show reasonable agreement with those determined within an upward burning plume six inches away from the combustion surface.

ACKNOWLEDGMENTS

This work is supported in part by the Center for Laser Applications at the University of Tennessee Space Institute and in part by Sandia National Laboratories. Sandia is a multi-program laboratory operated by Sandia Corporation, a Lockheed Martin Company, for the United States Department of Energy National Nuclear Security Administration under contract DEAC0494AL85000.

REFERENCES

1. Gill W, Cruz-Cabrera AA, Donaldson AB, Lim J, Sivanthu Y, Bystrom E, Haug A, Sharp L, and Surmick DM 2014 **Combustion diagnostics for analysis of solid propellant abort hazards: Role of Spectroscopy** *J. Phys.: Conf. Series* **548**, 012055 (10pp, in press).

2. Piehler TN, DeLucia FC, Munson CA, Homan BE, Miziolek AW, and McNesby KL, **Temporal Evolution of laser-induced breakdown spectroscopy spectrum of aluminum metal in different bath gasses** *Appl. Opt.* **44**, 3654-3660 (2005).

3. Mott Peuker J, Lynch P, Krier H, and Glumac N, **On AlO emission spectroscopy as a diagnostic in energetic materials testing**, *Propell. Expols. Pyrot.* **35,** 1-9 (2010).

4. Poletaev N I and Florko A V, **Spectral studies of the gas component of an aluminum dust flame**, *Combust. Explo. Shock* **44,** 437-443 (2008).

5. Tanguay V, Goroshin S, Higgins AJ, and Zhang F, **Aluminum particle combustion in high-speed detonation products**, *Combust. Sci. Tech.* **181,** 670-693 (2009).

6. Gallier S, Sibe F, and Orlandi O,**Combustion response of an aluminum droplet burning in air**, *Proc. Comb. Inst.* **33,** 1949-1956 (2011).

7. Lynch P, Krier H, and Glumac N, **Emissivity of aluminum oxide particle clouds: Application to pyrometry of explosive fireballs,** *J. Thermophys. Heat Tr.* **24,** 301-308 (2010).

8. Bucher P, Yetter RA, Dryer FL, Parr TP, and Hanson-Parr DM, **PLIF species and ratiometric temperature measurments of aluminum particle combustion in O_2, CO_2**

and N_2O oxidizers and comparsion with model calculations, *Proc. Comb. Inst.* **27,** 2421-2429 (1998).

9. Escot Boangera P, Davidenko D, Sarou-Kanain V, Chauveau C, and I Goekalp, **Experimental and numerical studies on the burning of aluminummicro and nanoparticle clouds in air**, *Exp. Therm. Flu. Sci.* **34**, 299-307 (2010).

10. Badiola C, Gill, RJ, and Dreizin EL, **Combustion characteristics of micron-sized aluminum particles in oxygenated environments**, *Combus. Flame* **158,** 2064-2070 (2011).

11. Goroshin S, Mamen J, Higgins A, Bazyn T, Glumac N, and Krier H, **Emission spectroscopy of flame fronts in aluminum suspensions**, *Proc. Comb. Inst.* **31,** 2011-2019 (2007).

12. Weismiller M0R, Lee JG, and Yetter RA, **Temperature measurements of Al containing nano-thermite reactions using multi-wavelength pyrometry**, *Proc. Comb. Inst.* **33,** 1933-1940 (2011).

13. Soo M, Julien P, Goroshin S, Bergthorson JM, and Frost DL, **Stabilized flames in hybrid aluminum-methane-air mixtures,** *Proc. Comb Inst.* **34,** 2213-2220 (2013).

14. Parigger CG and Hornkohl JO, **Computation of AlO $B^2\Sigma^+ \rightarrow X^2\Sigma^+$ emission spectra**, *Spectrochim. Act. A* **81,** 404-411 (2011).

15. Dors IG, Parigger CG, and Lewis J, **Spectroscopic temperature determination of aluminum moxide in laser ablation with 266-nm radiation**, *Opt. Lett.* **23,** 1778-1780 (1998).

16. Parigger CG, Woods AC, Surmick DM, Donaldson AB, and Height JL, **Aluminum flame temperature measurments in solid propellant combustion**, *Appl. Spectrosc.* **68,** 362-366 (2014).

17. Surmick DM, Parigger CG, Woods AC, Donaldson AB, Height JL, and Gill W, **Analysis of emission spectra of aluminum monoxide in solid propellant flame**, *Int. Rev. Atom. Mol. Phys.* **3,** 137-152 (2012).

18. Hornkohl JO, Parigger CG, and Nemes L, **Diatomic Hönl-London factor computer program**, *Appl. Opt.* **44,** 3686-3695 (2005).

19. Nelder JA and Mead R, **A simplex method for function minimization**, *The Comp. J.* **7,** 308-313 (1965).

20. Lagarias JC, Reeds JA, Wright MH, and Wright PE, **Convergence properties of the nelder-mead simplec method in low dimensions**, *SIAM J. Optim.* **9,** 112-147 (1998).

21. Boren CF and Huffman DR, **Absorption and scattering of light by small particles**, New York: Wiley (1983).

22. Stewart SM, **Blackbody radiation functions and polylogarithms**, *J. Quant. Spectrosc. Radiat. Transf.* **113,** 232-238 (2012).

23. Siewert CE, **An exact expression for the Wien displacement constant**, *J. Quant. Spectrosc. Radiat. Transf.* **26,** 467 (1981).

24. Height JL, Donaldson AB, Gill W, and Parigger CG, **Measurements in solid propellant**

plumes at ambient conditions, *Proc. ASME Int. Mech. Eng. Cong. Exp.,* Denver, CO (November 11-17, 2011) IMECE2011-62726 (6pp).

25. Yan ZX, Deng J, and Luo ZM, **A comparison study of the agglomeration mechanism of nano- and micrometer aluminum particles**, *Mater. Charac.* **61,** 198-205 (2010).